JOURNAL OF APPLIED ELECTROCHEMISTRY 25 (1995) 412–417

Potentiostatic study of the passivation of aluminium alloys in aqueous electrolyte media

M. ELBOUJDAINI, E. GHALI

Department of Mining and Metallurgy, Laval University, Quebec, Canada G1K 7P4

R. G. BARRADAS, M. GIRGIS

Department of Chemistry, Carleton University, Ottawa, Canada K1S 5B6

Received 5 March 1992; revised 24 November 1992

The anodic oxidation of Al 5083 and Al 6061 has been studied by steady state and transient polarization measurements in deoxygenated chloride solution containing sulphate ions at 22° C. Complementary to the electrochemical studies, techniques such as scanning electron microscopy (SEM) and X-ray photoelectron spectroscopy (XPS) were applied to investigate the morphological structure and chemical state of the electrode surface. The data suggests that a porous film of MgO and possibly Fe_2O_3 (for Al 6061) is formed on the electrode surface in addition to the aluminium oxide film (Al_2O_3). Some mechanisms for the growth of surface films on both alloys are discussed.

1. Introduction

In spite of the extensive investigations in the field of anodic passivation of aluminium, there have been relatively few fundamental electrochemical studies on the anodic behaviour of aluminium alloys in aqueous media using the techniques of cyclic voltammetry and potentiostatic pulses. Most of the previous studies have focused attention on the nature of the corrosion processes that occur on the electrode surface such as pitting, crevice corrosion or certain aspects of stress corrosion cracking [1]. Some experiments have been performed on steady-state anodization of high purity aluminium electrodes at high potentials in sulphuric, phosphoric, oxalic and propanedioic acids by means of potentiostatic and galvanostatic techniques [(2–5)]. Few attempts have been carried out to investigate the behaviour of aluminium alloys in aqueous media by applying constant potentials within the passive range [(6–8)]. No complete account has been given of the electrochemical behaviour of intermetallic compounds present in the structure of aluminium alloys [9]. Recently, Elboujdaini *et al.* [(10, 11)] investigated the electrochemical behaviour of some aluminium alloys in aqueous chloride and/or sulphate solutions by means of cyclic and linear sweep perturbations. They suggested a probable formation of a monolayer(s) of MgO and/or Al_2O_3 prior to the breakdown potential of each alloy. The purpose of this paper is to investigate the mechanism of growth of surface films on Al 5083 and Al 6061 alloys by means of a potential step method. The chemical composition was studied by X-ray photoelectron spectroscopy.

2. Experimental details

Aluminium alloys (5083 and 6061), with exposed surface area 1 cm^2, were used as working electrodes. The chemical composition of each alloy is described in Table 1. Prior to the electrochemical measurements, the electrodes were mechanically polished using a series of emery papers (grit 240 to 600) and finally polished with 0.3 μm abrasive alumina and dried with methanol. Graphite served as a counter electrode and all potential measurements were made with reference to a saturated calomel electrode (SCE).

The electrolytes of 3% NaCl (0.5 M) and 0.5 M NaCl–0.05 M Na_2SO_4 were prepared from BDH Aristar grade reagents. The solutions were degassed with 99.999% argon for 1 h before acquisition of data.

All experiments were conducted at 22 ± 1° C and involved potentiostatic control using conventional voltammetric systems (PAR models 173, 175 and 276) in conjunction with Hewlett Packard 2d-2 X–Y recorder.

The electrode was removed from the cell after stepping to the desired potential, rinsed with triply distilled water, vacuum dried and transferred immediately to the ultra high vacuum (u.h.v.) chamber with base pressure of 10^{-8} torr.

The morphology of the electrode surface was examined by means of a Jeol-2553 SEM. Surface analytical studies by X-ray photoelectron spectroscopy (XPS) were employed to examine and identify the nature of the passive layer using a VG Scientific Escalab Mk II instrument multifunction apparatus.

0021-891X

Table 1. Chemical composition of Al 5083 and Al 6061

Elements /wt %	*Al 5083*	*Al 6061*
Si	0.40	0.6
Fe	0.4	0.7
Cu	0.1	0.27
Mn	0.3–1.0	0.15
Mg	4.0–4.9	1.00
Cr	0.5–0.25	0.15–0.35
Zn	0.25	0.25
Ti	0.15	0.15
Others	0.15	0.15

3. Results and discussion

3.1. Corrosion potential

The polarization characteristics of Al 5083 and Al 6061 in deaerated 0.5 M NaCl–0.05 M Na_2SO_4 were produced potentiodynamically at a sweep rate of 16.7 mV min^{-1}. The corrosion potentials obtained for both electrodes were −850 and −700 mV, respectively. These values are lower than those observed for a pure aluminium electrode. This reflects the detrimental effect of magnesium iron containing phases on the corrosion process. These elements decrease the breakdown potential, enhance the anodic dissolution of the matrix and lower the hydrogen overpotential [(7, 9, 11, 12–14)].

3.2. Cyclic voltammetric studies

Typical cyclic voltammograms for pure aluminium and aluminium alloys in 3% NaCl at 22° C are shown in Figs 1 and 2, respectively. The potential was swept anodically from −1400 to −60 mV, reversed and swept cathodically back to −1400 mV. Unlike the voltammetric behaviour of the pure Al electrode, the voltammograms in the case of Al 5083 and 6061 electrodes were characterized by a minor peak (I) in the potential region of −900 to −800 mV. The presence of such a peak gives rise to the possible formation of monolayer(s) of aluminium oxide on the foreign particles, which are present in a high concentration in both alloys (4.5% by weight in Al 5083 and 1% in Al 6061). [11]. Surface analysis revealed the presence of magnesium. The scan was allowed to sweep anodically to the region of peak I and the electrode was then removed, dried and transferred to the u.h.v. chamber where the state of the surface was characterized by XPS. The spectra in the case of Al 5083, revealed the presence of peaks related to Mg: Mg2p (~ 51 eV), Mg2s (~ 91 eV and 1300 eV) and Mg KLL (305–315 eV). In addition, peaks related to 015 (550 eV) and Al2p (76 eV) were also detected. The location and shape of Mg2p and Al2p peaks (Fig. 3) indicate that the signals derive from oxide films [(15)]. Similar spectra were obtained for Al 6061.

The mechanism of particle removal as suggested by Nisancioglu *et al.* [(7, 8)] and by Mazurkiewicz [(9)] can be applied successfully to interpret the voltammetric behaviour of both alloys. The presence of electroactive magnesium in high content in both alloys may result in a high rate of cathodic activity (i.e., hydrogen evolution at the magnesium particle surfaces) and this leads, in neutral solutions, to the formation of alkaline diffusion layers localized

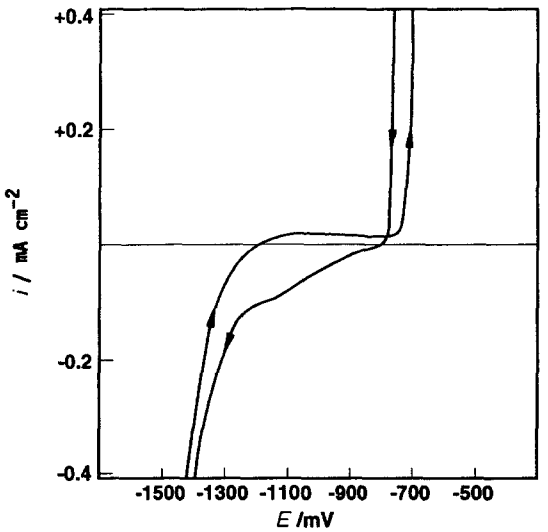

Fig. 1. Cyclic voltammogram for pure aluminium electrode in 3% NaCl; pH 7 at 25° C ($v = 5$ mV s^{-2}).

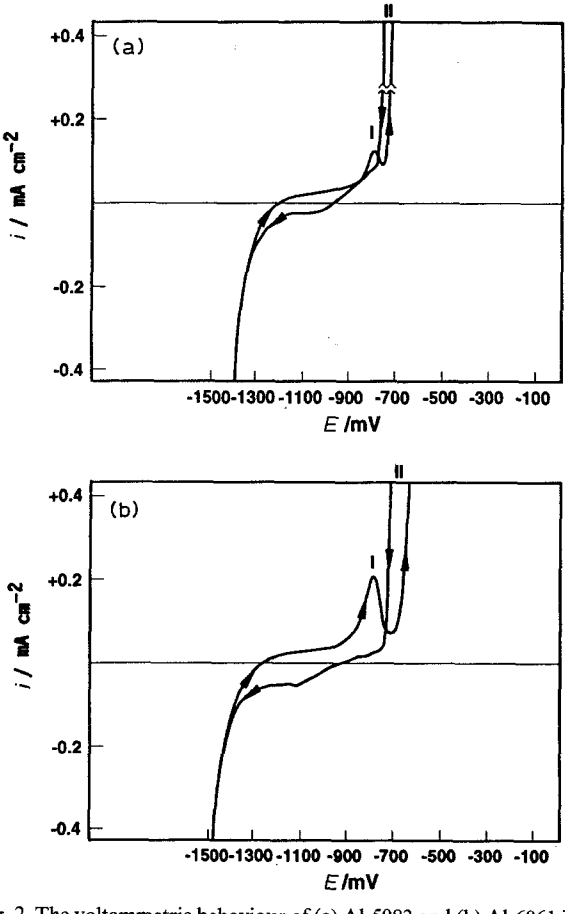

Fig. 2. The voltammetric behaviour of (a) Al 5083 and (b) Al 6061 in 3% NaCl; pH 7 at 22° C ($v = 50$ mV s^{-1}). (- - -) represents the voltammograms initiated from starting potentials greater than −1.5 V.

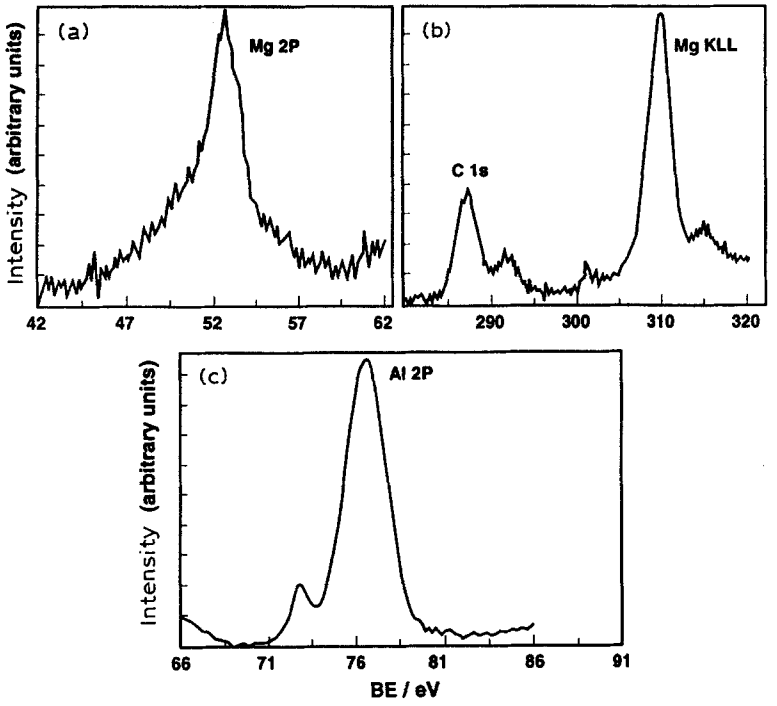

Fig. 3. (a) X-ray photoelectron spectra for the oxide film formed on Al 5083 in the region of peak I (see Figure 2) in 3% NaCl; (a), (b) and (c) represent the most characteristic peaks of the general spectrum.

around the particles. The pits are then formed around the matrix and may trap the alkaline catholyte. The removal of Mg-rich particles from the electrode surface occurs as a result of the dissolution of the matrix around the particles. As the scan progresses in the anodic direction, the cathodic activity ceases and a protective oxide film is reformed on the surface of the pit formed in place of the removed particle.

In the light of (i) the above–suggested mechanism, (ii) surface analysis conducted by the techniques of SIMS [(11)], and (iii) the absence of peak I in the case of the pure aluminium electrode, the presence of peak I may be ascribed to the formation of a Mg-rich phase. From the thermodynamic point of view, Mg^{2+} ions exist over the entire range of potentials applied in this study, thus, as a result of the vigorous hydrogen evolution at the starting potential, the sufficiently alkaline atmosphere in the vicinity of the magnesium particles results in the formation of a protective layer of $Mg(OH)_2$ and/or MgO. It is stated [(16)] that at pH 8.5, magnesium may be covered with a more or less protective oxide or hydroxide. To confirm the role of hydrogen, a cyclic voltammogram was produced by allowing the scan to sweep from a starting potential of −0.95 V to a final potential of −0.6 V. This resulted in a considerable decrease in the current density of peak I for both alloys. Foley [(1)] stated that magnesium can be incorporated into the corrosion product film on the surface of AlZnMg alloy (AA 7075-T6) in the form of MgH or MgH_2 compounds with hydrogen being produced by the reaction of aluminium and water.

The anodic current, which rises sharply at around −0.7 V, is indicative of a pitting process. It was interesting to note that continuous recycling at a sweep rate of $50\,mV\,s^{-1}$ in the potential range −1.5 to −0.7 V resulted in a considerable decrease in the anodic current in regions I and II. This may reflect growth of an oxide film on the electrode surface.

The addition of 0.05 M Na_2SO_4 to the 3% NaCl solution resulted in a lowering of the current density and a shift of the pitting potential in the anodic direction.

3.3. Potential step measurements

To study the process(es) taking place in regions I and II (shown in Fig. 2), the working electrode was held at −1.5 V for 1 min prior to stepping the potential into the region of interest. The majority of current transients were recorded over short periods of time (maximum period was 2 min) to minimize the impurity effects and the changes in the morphology of the surface. For a wide range of imposed potential steps, the transients exhibited different, but reproducible, *i–t* morphologies, thereby indicating that the surface changes were minimal over the testing period and/or the morphology of the surface changed in a reproducible manner [(17, 18)].

After the potential step into region I, a fast decrease in current density with time was observed, probably because of double layer charging. This was followed by formation of a peak current for Al 6061 and only in the presence of sulphate ions for Al 5083 (Figs 4 and 5). The "hump" observed in the transients is probably a result of oxide formation (MgO and Al_2O_3 as suggested earlier). It has been suggested by Thompson *et al.* [(19)] that, after an induction time, the growing film breaks, followed by preferential growth above the ridges of the metal (due possibly

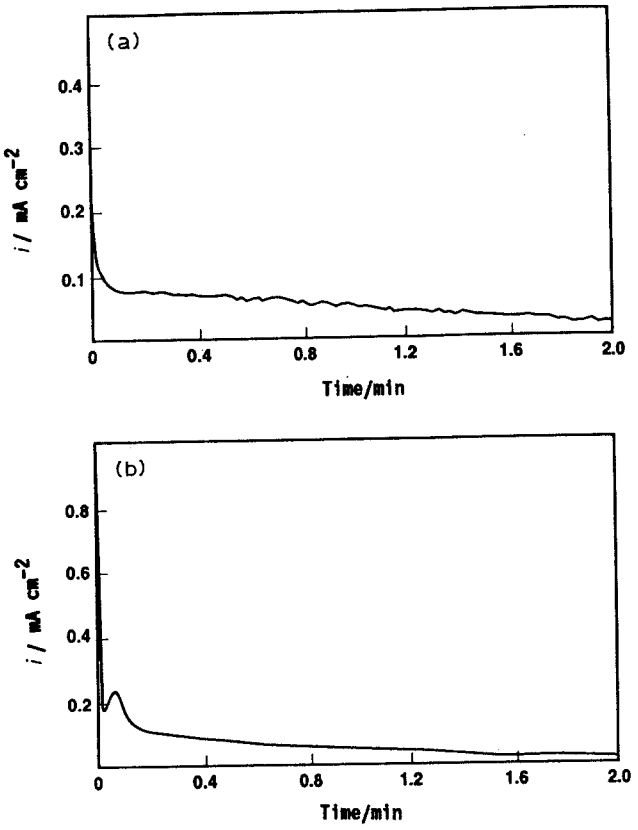

Fig. 4. Potentiostatic transient recorded for Al 5083 after pulsing the system to −900 mV SCE in (a) 3% NaCl and (b) 3% NaCl + 0.05 M Na_2SO_4; pH = 7 at 22° C.

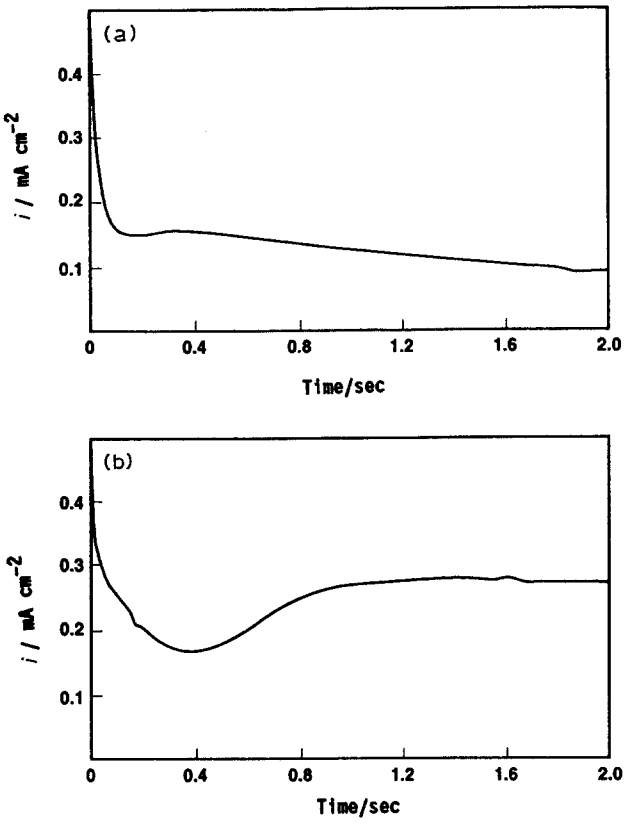

Fig. 5. Typical potentiostatic transient obtained for Al 6061 in (a) 3% NaCl and (b) in the presence of 0.05 M Na_2SO_4 after pulsing the system to −900 mV (SCE) at 22° C.

to the existence of a greater impurity-derived flaw density near the ridges compared with the more uniform regions between the ridges). Siejka and Ortega [(20)] postulated that Al^{3+} ejection at the film/electrolyte interface is followed by partial precipitation of solid alumina. The absence of a peak current in the case of Al 5083 alloy in Cl-containing solutions may be attributed to vigorous hydrogen evolution at the electrode surface upon the imposition of the initial potential, especially when it is considered that the matrix of Al 5083 contains a high percentage of electroactive metal particles (Mg and Fe) which may depolarize the cathodic reactions. This may result in retardation of the nucleation process. Careful examination of the i–t transient recorded for Al 5083 over a very short period of time (20 ms) revealed the presence of a small peak current formed after stepping the potential.

The analysis of the ascending branch of the i–t curve for Al 6061 (Fig. 5) showed that the dependence of the current on time was

$$I = Kt^3 \tag{1}$$

where K is a constant. This is characteristic of three-dimensional growth according to the geometric model developed by Armstrong *et al*, ([(21)]

$$I = nFK_2\left[1 - exp\frac{(-\pi M^2 K_1^2 A t^3)}{3p^2}\right] \tag{2}$$

where i the current (mA cm^{-2}), n is the number of electrons, F the Faraday constant and K_1 and K_2 are lateral and vertical growth constants (cm s^{-1}). A is the nucleation rate, M the molecular weight, t the time and p the density of the oxide film.

Stepping to various potentials within and beyond the limits of region I and II for Al 6061 resulted in a series of transients as shown in Fig. 6. Further analyses were performed from the current maximum i_m and t_m could be expressed as

$$I_m = \frac{nFK_2}{4} \tag{3}$$

$$t_m = \frac{3p^2 \ln 2}{\pi M^2 K_1^2 A} \tag{4}$$

The general tendency of the transient behaviour showed a greater dependence on i_m than on t_m for various imposed potentials (Table 2). This suggests that the vertical growth (Equation 3) of the film was affected more than the lateral growth and/or the nucleation rate (Equation 4).

Table 2. The values of i_{max} and t_{max} calculated for various i–t transients for Al 6061 in 3% NaCl + 0.05 M Na_2SO_4

Values	*Potential*/mV vs. SCE			
	−900	−850	−800	−700
i_{max}/mA cm^{-2}	2.58	4.98	7.87	10.3
t_{max}/s	1.2	0.59	0.45	0.5

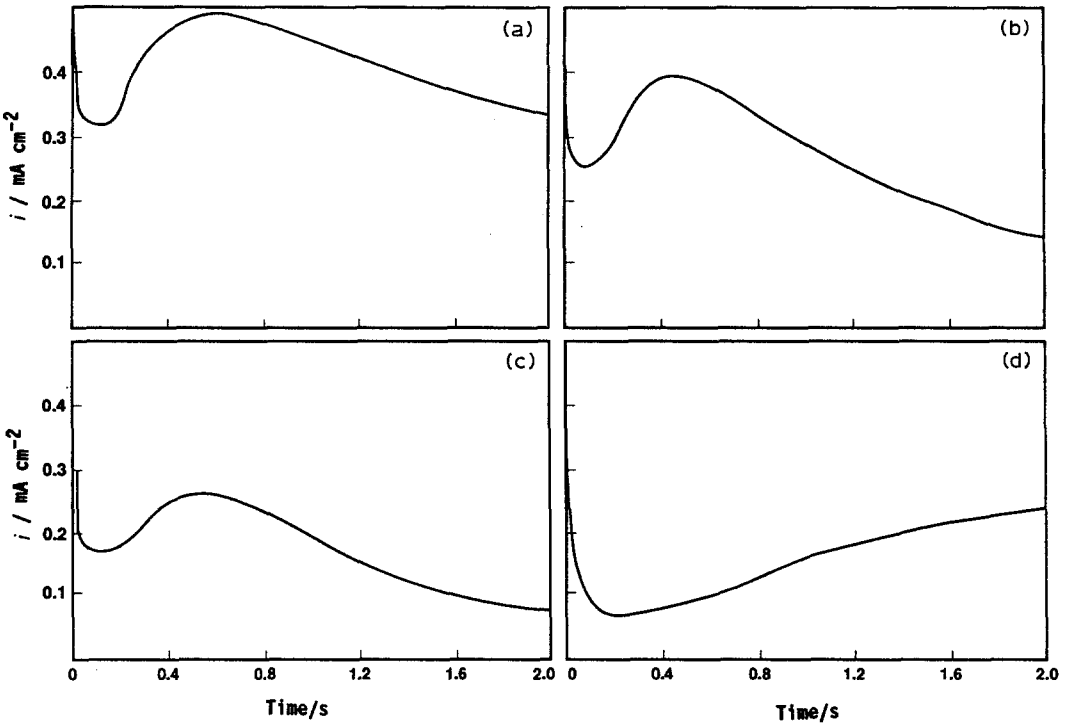

Fig. 6. Family of $i - t$ transients recorded for Al 6061 upon pulsing the system to various anodic potentials: (a) −850, (b) −800, (c) −750 and (d) −600 mV (SCE) in 3% NaCl + 0.05 M Na_2SO_4.

The potentiostatic experiments conducted for the pure aluminium electrode by stepping the system to anodic potentials in the region of the major dissolution/passivation process (≥ -700 mV) resulted in $i - t$ transients similar to that obtained for Al 5083, i.e. the film was formed via three-dimensional growth under influence of diffusion. This indicates that the nucleation and growth of the aluminium oxide film on both surfaces may proceed via the same mechanism. Such an observation is unusual since it might be expected that the particles in the matrix of Al 5083 would play a significant role on the nature of the nucleation and growth process as compared to the pure aluminium surface. This may indicate that the removal of the foreign particles leaves the Al 5083 surface bare so that the surface becomes similar to that of pure aluminium.

The role played by magnesium may also explain the general tendency of the observed high current density in the case of using Al 5083 as compared to Al 6061. The presence of magnesium may depolarize the hydrogen evolution reaction at the initial potential, so that protons penetrate the oxide layer, and hydrogen formed at the oxide surface leads to an eventual rupture of blisters in the protective oxide layer. The continuous excavation of the surface by Mg-rich phase removal may also lead to further porosity in the oxide film resulting in an increase in the anodic current. Table 3 shows the amount of charge calculated at different anodic potentials. The data reflect two observations: (i) the values are very large to account for two dimensional nucleation and growth mechanism and (ii) the values obtained for the pure aluminium electrode are similar to those for Al 5083. The latter observation is in agreement with the similarity of the transient behaviour for both electrodes. The amount of charge required to penetrate the surface was calculated as follows:

$$Q = 0.54\, nFK_2 \left[\frac{pM^2K_1^2A}{3p^2}\right]^{1/y} \qquad (5)$$

where y is a term related to the nucleation process. From the data shown in Table 3, it may be inferred that, up to an anodic potential of ≥ -800 mV, the charge calculated for both alloys are very close. This implies that both K_1, the film growth rate constant parallel to the electrode surface, and K_2, the rate constant vertical to the electrode surface, are controlled by aluminium only and are therefore the same. The significant change in the calculated values for both electrodes was clearly observed for potentials > -800 mV, where high values were reported for Al 5083. This may be explained in terms of a

*Table 3. The amount of charge (mC) calculated after pulsing the system to different anodic potentials in 3% NaCl**

E/mV(SCE)	*5083*	*6061*	*Pure Al*
−900	4.00	3.90	uc†
−850	6.00	5.10	uc†
−800	7.70	6.00	1
−750	5.45	4.32	3
−700	620.00	27.00	500
−650	2150.00	1310.00	1950
−600	2910.00	2430.00	3300

*The values in the presence of SO_4^{2-} ions were less than that calculated in the pure chloride medium, but the same tendency was observed.

†uc = unable to calculate.

porous film formation in the potential region of peak I for Al 5083, which permits further dissolution of Al^{3+} ions through the pores, with subsequent formation of an Al_2O_3 film on top of the initial porous layers. This would proceed through preferential nucleation sites and thus lead to irregular growth of the surface layer. The behaviour upon stepping to −750 mV for both electrodes resulted in a very interesting phenomenon; the charge (as shown in Table 3) reached a minimum value and then started to increase again at more positive potentials. This trend was confirmed by repeating the experiments several times. It seems that at this critical potential, some of the layers initially formed in region I are detached from the surface due to the massive penetration of Al^{3+} ions from the substrate surface prior to the nucleation of Al_2O_3. This phenomenon was not observed for the pure aluminium electrode since no film forms at potentials greater than −750 mV (see Fig. 1).

4. Summary

The electrochemical behaviour of Al 5083 and Al 6061 shows a marked difference from that observed for a pure aluminium electrode. The peak observed on the voltammograms prior to the breakdown potential is attributed to the influence of Mg and/or Fe-rich phases. This inference has been confirmed by XPS analysis. The potentiostatic behaviour at potentials in the range −1.5 to −0.6 V initially shows a marked current density decay with time, followed by a minimum, a maximum, and a steady-state current density. Numerical analyses for the rising portions of the transients show a similarity in behaviour between Al 5083 and the pure aluminium electrode. In general, the results show that the oxide films grow in three dimensions under diffusion control.

5. Acknowledgements

Two of us (E. G. and R. G. B.) are grateful for financial support from the Natural Sciences and Engineering Research Council of Canada. Surface analyses offered by the laboratories GRAPS, Laval University, are acknowledged with special thanks to Dr A. Adnot for scientific guidance.

6. References

[1] R. T. Foley, *Corrosion* **42** (1986) 277.
[2] P. L. I. Cabot and E. Perez, *Electrochim. Acta* **31** (1986) 319.
[3] *Idem, ibid.* **30** (1985) 1573.
[4] E. Palibroda, *ibid.* **23** (1978) 835.
[5] P. L. I. Cabot, F. A. Cantellas, E. Perez and J. Virgili, *ibid.* **30** (1985) 1035.
[6] F. P. Ford, G. T. Burstein and T. P. Hoar, *J. Electrochem. Soc.* **127** (1980) 1325.
[7] K. Nisancioglu, K. Y. Davanger and O. Strandmyr, *ibid.* **128** (1981) 1523.
[8] K. Nisancioglu, O. Lunder and H. Holtan, *Corrosion* **41** (1985) 247.
[9] B. Mazurkiewicz, *Corrosion Sci.* **23** (1983) 687.
[10] M. Elboujdaini, E. Ghali and A. Galibois, *J. Appl. Electrochem.* **18** (1988) 257.
[11] M. Elboujdaini, E. Ghali, R. G. Barradas and M. Girgis, *Corrosion Sci.* **30** (1990) 855.
[12] K. Goto, Y. Shimizu and G. Ito, *Trans. Nat. Res. Inst. Metals (Japan)* **22** (1980) 86.
[13] E. Mattsson, L. O. Gullman, L. Knutsson, R. Sundberg and B. Thundal. *Brit. Corros. J.* **6** (1971) 73.
[14] J. Zahavi, J. Yahalom, *J. Electrochem. Soc.* **129** (1982) 1181.
[15] C. D. Wagner, W. M. Riggs, L. E. Davis, J. F. Moulder, 'Handbook of X-ray Photoelectron Spectroscopy', (edited by G. E. Muilenberg), Perkin–Elmer Corp. Minnesota, (1979).
[16] R. K. Viswanadham, T. S. Sun, J. A. S. Green, *Met. Trans.* **11A** (1980) 85.
[17] D. D. MacDonald and B. Roberts, *Electrochim. Acta* **23** (1978) 557.
[18] C. Y. Chao, L. F. Lin and D. D. MacDonald, *J. Electrochem. Soc.* **128** (1981) 1187, 1194.
[19] G. E. Thompson, R. C. Furneaux, G. C. Wood, J. A. Richardson and J. S. Goode, *Nature* **272** (1978) 433.
[20] J. Siejka and C. Ortega, *J. Electrochem. Soc.* **124** (1977) 883.
[21] R. D. Armstrong, M. Fleischmann and H. R. Thirsk, *J. Electroanal. Chem.* **11** (1966) 208.